Polish J. Chem., **78**, 1753–1764 (2004)

Measurements of Interfacial Area in Helicoidal Reactor*

by S. Wroński and T. Ryszczuk

Faculty of Chemical and Process Engineering, Warsaw University of Technology,
ul. Waryńskiego 1, 00-645 Warszawa, Poland
Fax +48 22 825 14 40, tel. +48226606295, E-mail:wronski@ichip.pw.edu.pl

(Received March 1st, 2004; revised manuscript May 7th, 2004)

Interfacial area was measured in a helicoidal reactor for the two-phase gas-liquid flow, assuming plug flow. Measurements were accomplished using the method of oxygen chemical absorption in alkaline solutions of $Na_2S_2O_4$. Large values of the interfacial area were found. A correlation between changes in the interfacial area and changes in the flow structure within the reactor was observed.

Key words: gas-liquid flow, interfacial area, helicoidal flow

Helicoidal flow in an annular gap results from superposition of the axial and rotational flows caused by a rotational motion of an inner cylinder. This type of flow is commonly referred to in references as Couette-Taylor flow (CTF). For such a flow loss of stability is characteristic above a critical value of the rotational velocity of a rotor. Under an effect of inertial force, a secondary fluid motion appears in the form of cellular Taylor vortices [1]. Appearance of the Taylor vortices (Fig. 1) and combination of the axial flow with the rotational one result in that helicoidal the flow has the several features, those result in increasing interest in applying Couette-Taylor flow in different processes. Studies on the flow structure which account for effects of longitudinal and radial mixing have been presented in [2,3]. The authors found much greater importance of longitudinal mixing. In an assessment of the reactor performance they introduced a parameter [3]

$$\Phi = \frac{D_{ax}}{D_{trans}}$$

where: D_{ax} – coefficient of axial dispersion, D_{trans} – coefficient of dispersion in the other directions. According to the cited papers, depending on the reactor type, the estimated values of Φ amount for a tubular reactor with turbulent flow 100–150, for a turbulent flow through a particulate bed 50, for a stirred reactor 1, for a CTF reactor ≤ 0.1. From this comparison one can conclude that the CFT reactor has a very advantageous dynamic characteristics allowing to practically assume a plug flow prevailing in such type of reactor. Recently published papers offer suggestions for application of helicoidal flow in the following processes: photocatalytic reactions [4], polymerization reactions [5], reversed osmosis [6], precipitation [7], blood detoxication [8].

* Dedicated to Prof. Dr. Z. Galus on the occasion of his 70th birthday.

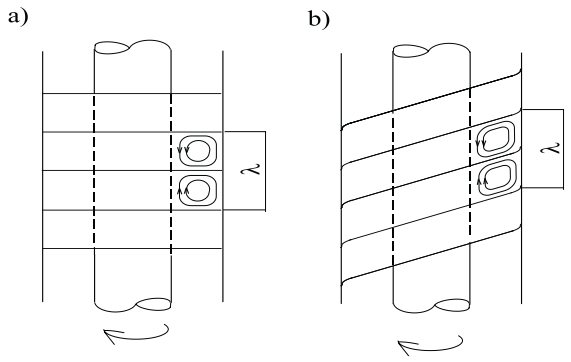

Figure 1. Cellular vortices of Taylor: a) toroidal ($Re_{ax} < 40$), b) spiral ($Re_{ax} > 40$).

Among the mentioned applications of helicoidal flow there are also those for multiphase systems. In the case of two-phase (gas-liquid) flow one can expect additional benefit from applying helicoidal flow, namely more intensive mass transfer between two phases and good conditions for dispersing gas phase at a low (unfavourable) ratio of gas and liquid phases.

Wroński *et al.* [9] and Dłuska *et al*. [10,11] studied this type of reactor and obtained high values of the volumetric mass transfer coefficients. Hubacz and Wroński [12] suggested a regime map for a two-phase flow in a horizontal CTF reactor.

In spite of publication of a number of papers on the application of the CTF reactor an evident lack of fundamental studies concerning hydrodynamic conditions of such type of a reactor can be observed.

The question of the interfacial area developed in the reactor that is an objective of the present paper has not so far been reported in the references. Therefore, such investigations have been conducted using chemical method based on absorption of oxygen in alkaline solutions of sodium dithionite was applied. From literature data on this method [13,14,15], it follows that within a wide range of sodium dithionite concentration reaction kinetics does not change significantly. Such a feature is of importance when interfacial area is determined in continuous flow reactors with widely changing reagent concentrations.

EXPERIMENTAL

Determinations of interfacial area were carried out in a helicoidal reactor. The main dimensions of the reactor are as follows: outer cylinder diameter $D_o = 37$ mm, length $L = 317$ mm, diameter of rotating cylinder $D_i = 20$; 26.5; and 34 mm. The outer and inner cylinders were made of plastic material.

The experimental apparatus is shown in Fig. 2. Helicoidal reactor (1) is its main part. The inner cylinder of the reactor is set into rotational movement by means of a driving gear consisting of a three-phase electrical motor (2) and a control device (3) enabling continuous regulation of the rotational

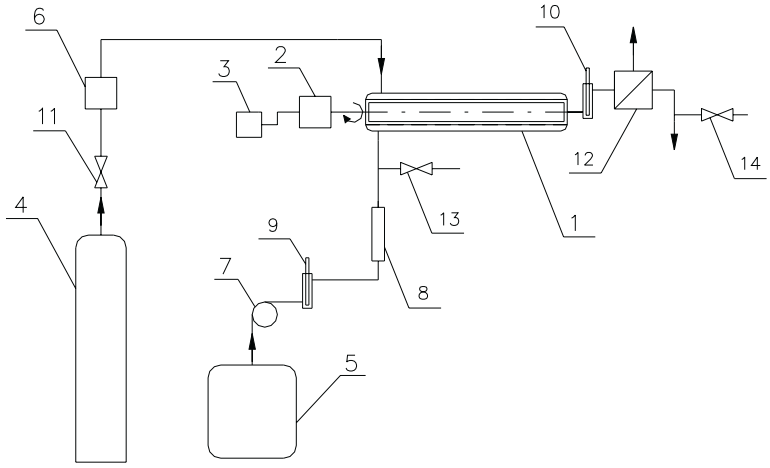

Figure 2. Experimental equipment: 1 – helicoidal reactor; 2 – motor; 3 – inverter; 4 – oxygen cylinder; 5 – vessel with alkaline solution of sodium dithionite; 6 – gas flow rate control device; 7 – peristaltic pump; 8 – rotameter; 9, 10 – termometers; 11 – reducing valve; 12 – separator; 13, 14 – three-way valves.

speed of the impeller. Absorbed gas (O_2) is taken from a pressure cylinder (4) with absorbing solution from a tank (5). Electronic flow-meter (6) is applied to control and measure gas flow rate. Liquid flow rate is controlled using a peristaltic pump (7) and measured with rotameter (8). The temperatures at the inlet and the outlet of the reactor are determined using thermometers 9 and 10. Separator (12) serves to separate the reaction mixture leaving the reactor. Samples for analyses are withdrawn by means of three-way valves 13 and 14.

Before accomplishing interfacial area determination, a solution of desired NaOH concentration was prepared. The solution was then saturated with nitrogen and then a predetermined amount of sodium dithionite was added. The obtained mixture and gas were fed into the reactor. After stabilizing process parameters (temperature, rotational speed of the rotor, liquid flow rate and the volumetric flow ratio of gas and liquid), liquid samples were withdrawn from the inlet and the outlet of the reactor to measure sodium dithionite concentration. The composition of the liquid phase was iodometrically analysed in presence of formaldehyde. The details of this method are given in [16]. Titration was carried out using a digital biurette and automatic pipette.

The initial concentration of NaOH was equal to 1 kmol/m^3. Concentration of sodium dithionite changed in the range of 0.01 to 0.2 kmol/m^3. Liquid mass flux varied between 2.7 and 100 kg/(m^2 ·s) while gas mass flux equalled 1.4–400 kg/(m^2·s), resulting in the volumetric flow ratio of gas and liquid from 0.125 to 1. Rotational speed of the rotor was changed from 0 to 2900 rpm. Owing to application of different rotor diameters (20–34 mm), the ratio of the impeller diameter to that of the outer diameter of the reactor could be obtained from 0.54 to 0.91. Temperature ranged from 20–30°C.

The range of hydrodynamic parameters was assumed based on a predicted range of a real reactor performance, *i.e.* large residence time and relatively small gas holdup.

The chemical method based on absorption of oxygen in alkaline solutions of sodium dithionite was applied. This method of determination of interfacial area in gas-liquid contactors was suggested by Jhaveri and Sharma [17,18], Sahay and Sharma [19], and Joshi and Sharma [20]. Camacho *et al*. [13,14,15] established that within the following range of parameters

$$0.005 \le \left[S_2O_4^{2-}\right] \le 0.2;\ 293 \le T \le 318;\ 2\cdot 10^4 \le P_{O_2} \le 10^5;\ pH \ge 8 \tag{1}$$

oxidation of sodium dithionite with molecular oxygen described as follows:

$$S_2O_4^{2-} + O_2 + 2OH^- \rightarrow SO_3^{2-} + SO_4^{2-} + H_2O \tag{2}$$

undergoes within fast reaction regime and is of zero'th order with respect to oxygen concentration and 1.5-th order with respect to sodium dithionite concentration

$$r = k\left[S_2O_4^{2-}\right]^{1.5} \tag{3}$$

$$k = 3.22 \cdot 10^5 \exp\left(-\frac{4250}{T}\right) \tag{4}$$

Since the publications of Camacho *et al*. [13,14,15] are the most recent reference data on this reaction, they were assumed as most reliable.

Application of a chemical method in determining interfacial area for the gas-liquid system in helicoidal reactor is based on the theory of absorption with simultaneous chemical reaction in the liquid phase [21,22]

$$A(g) + zB(l) \rightarrow products \qquad (-r_A) = kC_A^n C_B^m \tag{5}$$

According to the theory, if gas mass-transfer resistance can be neglected the following expression can be derived for the product of the molar flux of component A and the interfacial area if gas mass-transfer resistance can be neglected

$$N_A a = \sqrt{1 + Ha^2}\, k_L^* a\left(C_{Ai} - \frac{C_{A0}}{1 + Ha^2}\right) \tag{6}$$

if a flat concentration profile of component B in vicinity of the interface can be assumed.

$$Ha = \sqrt{\frac{\frac{2}{n+1} D_A k C_{B0}^m C_{Ai}^{n-1}}{\left(k_L^*\right)^2}} << \frac{C_{B0}}{zC_{Ai}} \tag{7}$$

For a fast reaction Ha ≥ 3, $C_{A0} = 0$ and the molar flux of component A reduces into

$$N_A a = \sqrt{\frac{2}{n+1} D_A k C_{B0}^m C_{Ai}^{n+1}}\, a \tag{8}$$

Eq. (8) can be used in determining interfacial area by measuring $N_A a$ and knowing kinetic parameters of the reaction, diffusivity and solubility of component A.

Taking into account that oxidation of sodium dithionite in alkaline solutions with molecular oxygen undergoes in the regime of fast reaction and assuming 1.5-th order with respect to dithionite and zeroth order with respect to oxygen in such a reaction, one can derive from Eq. (8)

$$N_{O_2} a = \sqrt{2kD_{O_2}\left[O_2\right]\left[S_2O_4^{2-}\right]^{1.5}}\, a \tag{9}$$

On the other hand, from Eq. (2) it follows that

$$N_{O_2} a = -u_L \frac{d\left[S_2O_4^{2-}\right]}{dL} \tag{10}$$

After separation of variables and integration, we will obtain from Eqs. (9) and (10) an expression that enables to calculate the interfacial area

$$a = \frac{4u_L\left(\left[S_2O_4^{2-}\right]_{inlet}^{0.25} - \left[S_2O_4^{2-}\right]_{outlet}^{0.25}\right)}{(2k)^{0.5}\sqrt{D_{O_2}\left[O_2\right]_i}\,L} \tag{11}$$

where $L/u_L = t$ – liquid residence time in the reactor.

Eq. (11) is valid for a reactor with plug flow that prevails in the helicoidal reactor. In view of the comments given in point 1 assumption of plug flow seems to be justified. The values of oxygen diffusivity in the liquid and oxygen concentration at the interface were substituted in Eq. (11) as the arithmetic averages from the values at the inlet and the outlet of the reactor.

In estimating oxygen diffusivity in the aqueous solutions of electrolytes, an equation due to Ratcliff and Holdcroft [23] was used

$$D_{O_2} = D_0\left(1 - \sum_i \varepsilon_i C_i\right) \tag{12}$$

where C_i is molar concentration of the *i*-th salt [kmol/m^3], D_0 – oxygen diffusivity in water [m^2/s], ε_i – characteristic constant for the *i*-th salt [dm^3/mol] that is practically independent of temperature.

Values of ε_i were given by Hikita et al. [24]

$$\varepsilon_{Na_2S_2O_4} = 0.204;\ \varepsilon_{Na_2SO_4} = 0.232;\ \varepsilon_{Na_2SO_3} = 0.25;\ \varepsilon_{NaOH} = 0.138 \tag{13}$$

In estimating oxygen diffusivity in water Stokes-Einstein equation with constants suggested by Himmelblau [25] was taken

$$\frac{D_0\mu}{T} = 7.22\cdot 10^{-15} \quad \text{N/K} \tag{14}$$

Oxygen concentration at the interface can be determined from the Henry's law

$$\left[O_2\right]_i = H\cdot p_{o_2,i} \tag{15}$$

where: H – Henry's law constant [kmol/(m$^3\cdot$ Pa)]; $p_{O_2,i}$ – oxygen partial pressure at the interface [Pa]; $\left[O_2\right]_i$ – oxygen concentration at the interface [kmol/m^3].

The Henry's law constant for the system oxygen-aqueous solutions of electrolytes can be estimated from the following expression

$$\log\left(\frac{H}{H_0}\right) = \sum_i h_i I_i \tag{16}$$

where: H_0 – Henry's law constant for the system oxygen-water; I_i – ionic strength of the *i*-th salt; h_i – contribution of the *i*-th electrolyte [m^3/kmol].

Values of the Henry's law constant for the system oxygen-water were determined from an equation given by Moniuk *et al*. [26]

$$H_0 = \frac{\alpha_B}{R_g\cdot T_0} \tag{17}$$

where: R_g – gas constant [J$\cdot$kmol$^{-1}\cdot$K^{-1}]; T_0 = 273.15 [K]; α_B – Bunsen coefficient, which can be determined from the following expression

$$\alpha_B = 0.049 - 1.335\cdot 10^{-3}\cdot t_L + 2.759\cdot 10^{-5} t_L^2 - 3.235\cdot 10^{-7}\cdot t_L^3 + 1.614\cdot 10^{-9}\cdot t_L^4 \tag{18}$$

where t_L – liquid temperature [°C].

Ionic strength of a given electrolyte was calculated from the familiar expression

$$I_i = \frac{1}{2}\sum_j c_j z_j^2 \tag{19}$$

where: c_j – concentration of the j^{th} ion [kmol/m^3]; z_j – absolute charge of the j^{th} ion.

Values of h for the subsequent electrolytes at several temperatures, estimated by Hikita *et al*. [24] are listed in Table 1.

Table 1. Dependence of the coefficient h on temperature for $Na_2S_2O_4$, Na_2SO_4, Na_2SO_3 and NaOH.

Temp. [°C]	h [dm^3/mol]			
	$Na_2S_2O_4$	Na_2SO_4	Na_2SO_3	NaOH
15	0.148	0.148	0.122	0.188
17.5	0.145	0.145	0.119	0.185
25	0.134	0.134	0.108	0.174
35	0.12	0.12	0.094	0.16

RESULTS AND DISCUSSION

The results of interfacial area measurements were presented as a function of rotational speed of impeller (N), volumetric flow rates of gas and liquid (β), liquid velocity (G) and the ratio of the inner and outer cylinder diameter (η).

The ratio, β, represents a nominal holdup value, calculated on the basis of the volumetric flow rates of both phases at the inlet to the reactor. Because of plug flow in both phases and the vortex structure, assumption of the lack of slip between the phases seems to be fully justified. It can be seen that the interfacial area depends much on process parameters such as rotational speed of impeller, the volumetric ratio of gas and liquid and the ratio of the inner and outer cylinder diameter, while liquid flow rate is of less importance.

Fig. 3, 4, 5 presents selected results of the interfacial area measurements. All obtained experimental data of the interfacial area was published in [27].

Diagrams a = f(N) are similar for all hydrodynamic conditions. It seems then justified to assume that these changes are dependent on hydrodynamic regime of helicoidal flow.

Error bars for the results of one of the experimental series, shown earlier in Fig. 3, are demonstrated in Fig. 6. It is seen that replication of measurements at the same operational conditions do confirm that reproducibility of the applied method is satisfactory since the deviations from a mean values do not exceed 15%.

Hubacz and Wroński [12] carried out investigations on the flow structure using a visualization method. Based on their own observations they suggested a map of the flow structures as a function of rotational speed, as well of energy dissipated by the rotational motion.

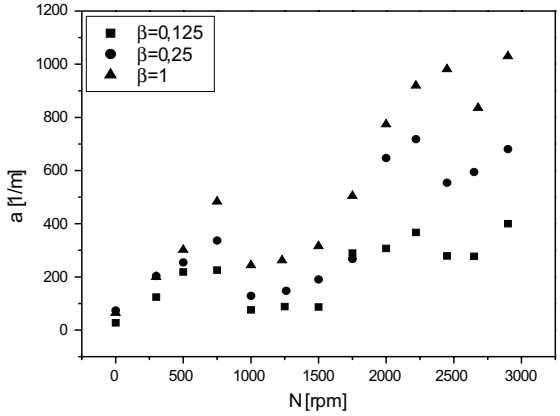

Figure 3. Dependence of interfacial area on rotational speed of impeller at different values of β for η = 0.54 and G = 11 kg/(m^2·s).

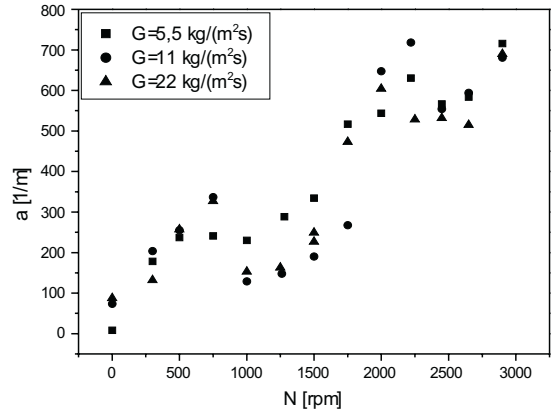

Figure 4. Dependence of interfacial area on rotational speed of impeller at different values of G for η = 0.54 and β = 0.25.

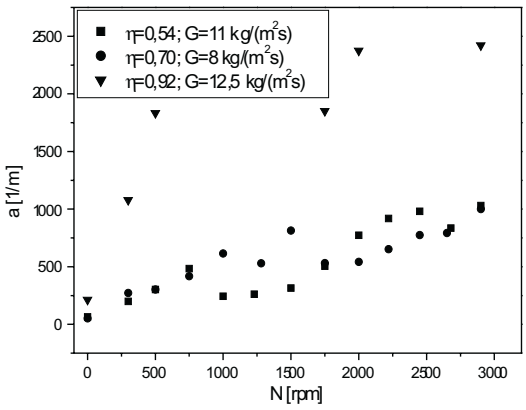

Figure 5. Dependence of interfacial area on rotational speed of impeller at different values of η for β = 1.

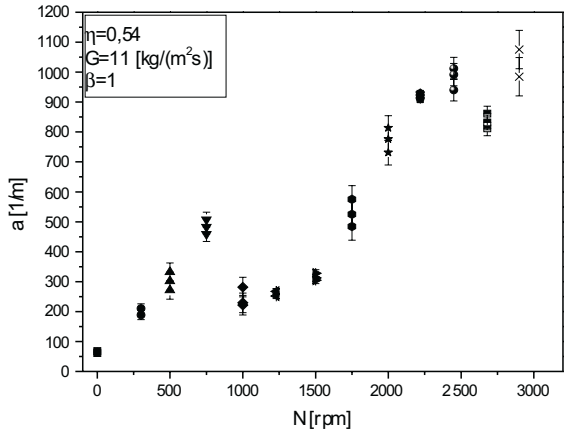

Figure 6. Reproducibility of data.

As an example, a map of the flow structures versus rotational speed of impeller is shown in Fig. 7. In the regions 1a, 1b, 1c, and 2a a stratified or slug flow are dominating while regions 2b and 2c are characterized by a transitional flow structure where two-phase cell vortices are present. In region 3 distinct, independent and – at the same time – parallel vortices are evident, with dominating liquid or gas phases. The results of interfacial area measurements indicate a univocal dependence of changes in interfacial area separation on the flow structure in the reactor. A coupling between changes of interfacial area with the rotational speed of impeller (Figs. 3, 4, 5) with the map of flow structures (Fig. 7) seems to be evident. Since a dependence of interfacial area on the rotational speed of impeller is not a monotonic function, generalization of the obtained results is a complex problem, requiring extensive experimental and simulation studies.

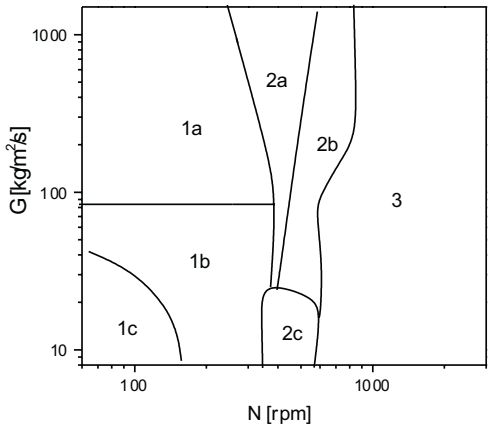

Figure 7. Map of flow regions (1a – SL (Slug flow); 1b – TR1 (Transition flow); 1c – ST (Stratified flow); 2a – DSL (Disturbed Slug flow); 2b – TR2 (Transition Regime); 2c – PE (Periodical flow); 3 – HR (High Rotation flow)).

It is now possible to combine changes in the character of curves describing the dependence of interfacial area with the energy dissipated by the rotational motion. One can conclude that interfacial area, a, first increases due to intensification of mixing (regions 1) until a transition structure (regions 2) is attained. Then, as a result of the ordered flow structure (phase segregation), it decreases more or less. Further increase in the rotational speed of rotor leads to changes in the liquid and phase vortex structures (region 3), then finally the vortices collapse and a turbulent flow structure is formed, in consequence yielding significant enlargement of the interfacial area. At smaller values of η, a transition from the stratified or slug regions (1) into the transition regions (2) also results in a decrease of interfacial area.

It is generally assumed that the best way in correlating the experimental data on the two-phase flows is to relate them to the values of dissipated energy per unit volume of the mixture. Since this parameter can be expressed as a function of the appropriate dimensionless numbers [28], as examples, the obtained results for a narrow and a wide gap were correlated in form of a function $a = f(Re_{rot})$, *cf*. Figs. 8 and 9. For a wide gap ($0.5 < \eta < 0.9$), a limiting value of $(Re_{rot})_1$ for transition from region 1 to region 2 is equal to about 8000, while analogous transition from region 2 to 3 $(Re_{rot})_2$ corresponds to *ca*. 27500. For a narrow gap ($\eta > 0.9$), the corresponding value of $(Re_{rot})_1$ amounts *ca*. 3500 while a limiting value of $(Re_{rot})_2$ has not been observed. Dependences of $a = f(Re_{rot})$ are located in a reasonable way, *i.e.* they indicate a dependence on β, such that at higher values of β we get higher values of the interfacial area. Previously mentioned small effect of the flow rate, G, is evident.

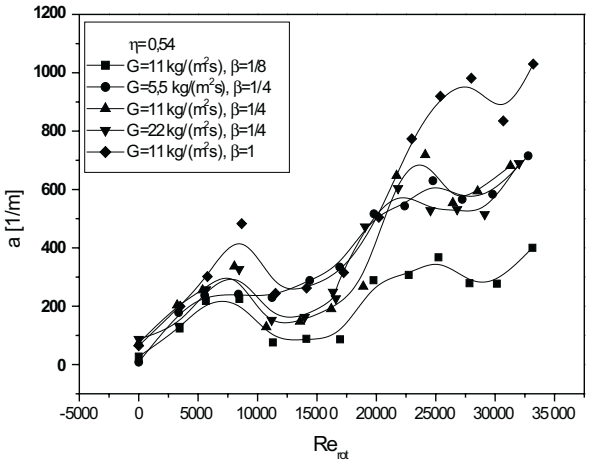

Figure 8. Dependence of interfacial area on rotational Reynolds number for $\eta = 0.54$.

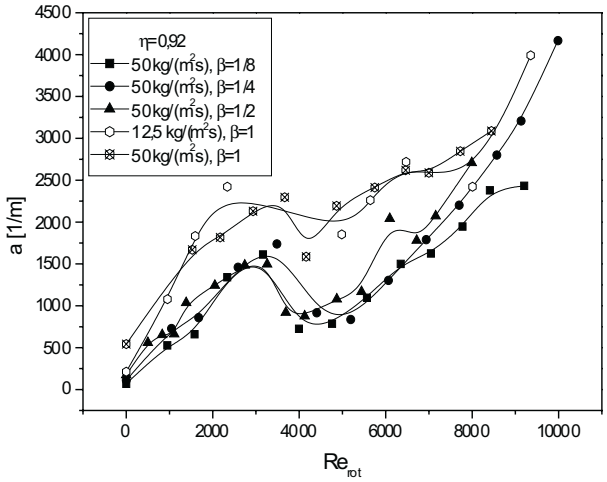

Figure 9. Dependence of interfacial area on rotational Reynolds number for $\eta = 0.92$.

CONCLUSIONS

1. Measurements of interfacial area, a, in the liquid-gas system were carried out using a method of chemical absorption of oxygen in alkaline solutions of sodium dithionite, assuming plug flow. The values of a are dependent on the rotational speed of rotor and/or the dissipated power.
2. Changes in the values of interfacial area as a function of the fundamental parameter, which is here energy dissipated in the rotational motion, univocally indicates that interfacial area between the phases depends on the system hydrodynamics.
3. The obtained values of interfacial area were correlated with the results of visual investigations of the CTPF reactor. Dependence of changes in the values of interfacial area on the flow structure in the reactor was proved. This makes it possible to suggest a hydrodynamic model of the reactor for three fundamental regions: a. cocurrent gas-liquid slug flow (regions 1 on the map); b. two-phase flow with vortices (concept of continuos stirred tank reactors in series) (regions 2); c. ring flow of parallel vortices of liquid and gas phases (region 3) [29].

These are the relevant conclusions when the reactor may be implemented to carry out complex reactions (selective, consecutive, *etc*.).

Notation. a – interfacial area related to a unit volume of reactor [1/m]; C – molar concentration [kmol/m^3]; d – annulus width [m]; d_m – mean bubble diameter [m]; D_A – diffusivity of the absorbed component in the liquid phase [m^2/s]; D_{ax} –axial dispersion coefficient [m^2/s]; D_{O_2} – oxygen diffusivity in the liquid phase [m^2/s]; D_i – rotor diameter [m]; D_o – outer cylinder diameter [m]; D_{trans} – transversal dispersion coefficient, [m^2/s]; G – mass flux [kg/(m^{2}s)]; h_i – contribution of the ith electrolyte to the Henry's law constant for the oxygen-water system [m^3/kmol]; H – Henry's law constant [kmol/m^{3}Pa];

Ha – Hatta number; I – ionic strength of solution [kmol/m^3]; k – reaction rate constant [m^{1,5}/(mol^{0,5}s)]; k_L – mass transfer coefficient [m/s]; k_L^* – mass transfer coefficient with chemical reaction [m/s]; L – length of reactor [m]; m – reaction order with respect to component B; n – reaction order with respect to component A; N – rotational speed of impeller [rpm]; N_A – molar flux of absorbed component A [kmol/m^{2}s]; $[O_2]_i$ – oxygen molar concentration at the interface [kmol/m^3]; P_{O_2} – oxygen partial pressure [Pa]; r – reaction rate [kmol/(m^{3}s)]; R_1 – radius inner cylinder [m]; $\mathrm{Re}_{ax} = \frac{u2d\rho}{\mu}$ – axial Reynolds number; $\mathrm{Re}_{rot} = \frac{\varpi 2d\rho}{\mu}$ – rotational Reynolds number; R_g – gas constant [J·kmol^{-1} ·K^{-1}]; t_L – temperature [°C]; T – absolute temperature [K]; u_L – liquid superficial velocity [m/s]; z – stoichiometric coefficient; z_j – absolute charge of the jth ion; $\left[S_2O_4^{2-}\right]$ – sodium dithionite concentration [kmol/m^3]; α_B – Bunsen coefficient given by Eq. (18); β – volumetric flow ratio of gas and liquid at the reactor inlet; ε – constant in Eq. (12) [m^3/kmol]; $\eta = D_i/D_o$ – ratio of the rotor and outer cylinder diameters; μ – viscosity [Pa · s]; ω – angular velocity of the inner cylinder [1/s].

REFERENCES

1. Taylor G.I., *Philos. Trans. R. Soc*., London, ser. A223, 243 (1923).
2. Desmet G., Verelst H. and Baron G.V., *Chem. Eng. Sci.*, **51**, 1287 (1996).
3. Desmet G., Verelst H. and Baron G.V., *Chem. Eng. Sci.*, **51**, 1299 (1996).
4. Sczechowski J.G., Koval C.A. and Nobel R.D., *Chem. Eng. Sci.*, **50**, 3163 (1995).
5. Kataoka K., Ohmura N., Kouzu M., Simamura Y. and Okubo M., *Chem. Eng. Sci.*, **50**, 1409 (1995).
6. Lee S. and Lueptow R.M., *J. Membrane Science*. **192**, 129 (2001).
7. Jung W.M., Kang S.H., Kim W.S. and Choi C.K., *Chem. Eng. Sci.*, **55**, 733 (2000).
8. Ameer G.A., Grovender E.A., Obradovic B., Cooney C.L. and Langer R., *AIChE Journal*, **45**, 633 (1999).
9. Wroński S., Dłuska E., Hubacz R. and Molga E., *Chem. Eng. Sci.*, **54**, 2963 (1999).
10. Dłuska E., Wroński S. and Hubacz R., *Chem. Eng. Sci.*, **56**, 1131 (2001).
11. Dłuska E., Wroński S. and Ryszczuk T., Mass transfer and interfacial area in gas-liquid Couette-Taylor flow reactor, 6th World Congress of Chemical Engineering, Melbourne, 23–27 September 2001.
12. Hubacz R. and Wroński S., Horizontal Couette-Taylor flow in two-phase gas-liquid system; flow patterns, *Experimental Thermal and Fluid Science* (accepted to print).
13. Camacho F., Paez M.P., Blazquez G. and Garrido J.M., *Chem. Eng. Sci.*, **47**, 4309 (1992).
14. Camacho F., Paez M.P., Blazquez G., Jiminez M.C. and Fernandez M., *Chem. Eng. Sci*., **50**, 1181 (1995).
15. Camacho F., Paez M.P., Jiminez M.C. and Fernandez M., *Chem. Eng. Sci*., **52**, 1387 (1997).
16. Committee on Analytical Methods, *Am. Dyestuff Reptr.*, **46**, 443 (1957).
17. Jhaveri A.S. and Sharma M.M., *Chem. Eng. Sci.*, **23**, 1 (1968).
18. Jhaveri A.S. and Sharma M.M., *Chem. Eng. Sci.*, **23**, 669 (1977).
19. Sahay B.N. and Sharma M.M., *Chem. Eng. Sci.*, **28**, 2245 (1973).
20. Joshi J.B. and Sharma M.M., *Can. J. Chem. Engng.*, **55**, 683 (1977).
21. Danckwerts P.V., Gas-Liquid Reactions, McGraw Hill, New York 1970.
22. Charpentier J.C., Mass transfer rates in gas-liquids absorbers and reactors. Advances in Chemical Engineering, Eds. Drew T.B., Cokelet G.R., Hoopes J.W.Jr., Vermeulen T., 11, 1 (1981). Academic Press, New York.
23. Ratcliff G.A. and Holdcroft J.G., *Trans. Inst. Chem. Engrs*., **41**, 315 (1963).
24. Hikita H., Ishikawa H., Sakamoto N. and Esaka N., *Chem. Eng. Sci.*, **33**, 392 (1978).
25. Himmelblau D.M., *Chem. Rev.*, **64**, 527 (1964).
26. Moniuk W., Pohorecki R. and Zdrójkowski A., *Reports of the Faculty of Chemical and Process Engineering at the Warsaw University of Technology*, **24**, 177 (1997).

27. Ryszczuk T., Ph. D. Thesis (in Polish), Faculty of Chemical and Process Engineering, Warsaw University of Technology, 2004.
28. Hubacz R., Ph. D. Thesis (in Polish), Faculty of Chemical and Process Engineering, Warsaw University of Technology, 2003.
29. Wroński S., Dłuska E. and Woliński J., Oxidation of the organic liquids in helical reactor; modelling of the reactors performance, *Polish J. Chem. Technol*. (to be published).